Mathematical Modelling of Chronic Drug Infusion for Toxicity Assessment.

Áine Norton[1], Jean Sathish[1], Steven Webb[1], Leon Aarons[2], Kylie Beattie[3], Radhia Eljazi[5], Natalie Pearson[3], Rajith Rajoli[1], Denis Reddyhoff[6], Marco Siccardi[1] & Dominic Williams[1]

[1]MRC Centre for Drug Safety Science, Department of Molecular & Clinical Pharmacology, University of Liverpool, Liverpool, UK (*Problem Presenter*)
[2]School of Pharmacy and Pharmaceutical Sciences, University of Manchester, Oxford Road, Manchester, UK.
[3]Computational Biology, Department of Computer Science, University of Oxford, UK
[4]Oxford Centre for Industrial and Applied Mathematics , Mathematical Institute, University of Oxford, UK
[5]Mathematical and Computer Sciences Department, Heriot Watt University, Edinburgh, UK
[6]Department of Mathematics, Loughborough University, Loughborough, UK

UK Mathematics-in-Medicine NC3Rs Study Group 2013

Abstract

The rapid *in vivo* elimination of drugs in rodents results in qualitative and quantitative differences in pharmaco-toxicological endpoints and confounds comparisons to the human setting. A rodent model of chronic intravenous infusion (CII) has been developed with the aim of being more representative of the human situation and to act as a tool to gain a mechanistic understanding of cellular events in disease progression. In a previous CII study, paracetamol (APAP) was administered to male *Wistar* Hannover rats (HsdHan:WIST) at 36 mg/kg/hr for 48 hr with the aim of achieving steady-state drug levels. However, steady-state was not achieved. There was an initial rising phase, peaking at 30 hr and a more rapid decreasing phase, indicative of an adaptive response. Previous modelling approaches both under-predicted the drug-serum level and failed to replicate drug- serum profile, as adaptive responses were not taken into account.

Development of the mathematical model involved the coupling of a reduced Ordinary Differential Equation (ODE) model with a physiologically based pharmacokinetic (PBPK) model by an equation describing the level of APAP in the media, in order to develop a more detailed model of paracetamol interaction. Through this model various parameters could be altered, based on biologically plausible scenarios to gain an insight into which adaptive response may be linked to the decrease in paracetamol concentration. Three scenarios for an adaptive response were investigated to see if any resulted in an eventual decrease in APAP concentration instead of steady-state; (1) non-linear glutathione (GSH) production on *N*-acetyl-*p*-benzoquinone imine (NAPQI) concentration, (2) altered transport of metabolites from cell due to increasing NAPQI concentration and (3) increased expression of CYP450s.The first two scenarios did not prove effective however by increasing CYP450 expression we were able to produce a decrease in APAP concentration after a certain time, which, with the inclusion of a time delay, may smooth out the model to produce more realistic results.

1. Introduction

1.1 Introduction to Adverse Drug Reactions (ADR)

Adverse drug reactions (ADRs) are a major clinical concern and large contributors to patient morbidity and mortality [1]. A U.S. meta-analysis found an estimated 6.7 % of hospitalised patients suffered an ADR, of which 5 % were fatal [1]. In a separate retrospective analysis of new chemical entities approved for use in the U.S. between 1975 and 1999, the potential for such ADRs was observed in 16 out of 548 (2.9 %) of the compounds and consequently withdrawn, with the liver being the organ most often affected [2]. Drug-induced liver injury is responsible for greater than 50 % of acute liver failure cases in the US, with paracetamol (*N*-acetyl-*p*-aminophenol, APAP) being the leading cause of acute liver failure [3]. Drug withdrawal during development or once in the clinic is very costly to industry, with an estimated €2B/p.a. spent on toxicity testing [4]. In addition, just under 400, 000 animals were used in toxicity testing in Great Britain in 2011 [5]. Thus, there is both a financial and moral imperative to improve methods for screening compounds for the potential to cause such ADRs and remove them from drug development at an earlier stage. A mechanistic understanding of the molecular and cellular events that culminate in whole organ toxicity underpins the advancement of such novel drug safety assessment strategies. Consequently the development of innovative tools which give us greater insight into these processes are crucial.

1.2 Toxicology testing in the 21st Century

The safety testing strategy for new chemical entities has remained largely the same over the last 50 years despite an obvious need for improvement due to the high incidence and lack of sensitivity in detection of ADRs. In a retrospective analysis of pharmaceuticals identified to cause clinical toxicity, 39/91 were not predicted from *in vivo* toxicity testing [6]. Multiple factors may be responsible for this disparity but toxicity tests which take account of these differences are often lacking. It is well known that human and animal differ in the way they deal with and are exposed to chemicals including; absorption, distribution, metabolism and excretion (ADME), life span, environmental factors (nutrition, general health, co-medication, etc.), etc. All of which confound the development of an ideal test system. One example of this is the intrinsic differences between animal and man with respect to how drug levels in the blood are maintained, where rodents are much more rapid eliminators than humans [7]. Gaining an understanding of the impact of these differences on toxicity is limited in current models for safety testing. Specifically and with regard to this report, the rapid *in vivo* elimination of drugs in rodents results in qualitative and quantitative differences in pharmaco-toxicological endpoints and confounds comparisons to the human setting. It is unlikely that one test system will be capable of dealing with all these factors but a more integrated process may aid in

stratifying toxicity testing, with a downstream consequence being a reduction in numbers of animals used.

1.3 Paracetamol as a representative hepatotoxicant

Drug-induced liver injury (DILI) is one of the leading causes of ADR, attributed to the livers role in the metabolism and biotransformation of drugs [8]. One compound which is a leading cause of acute liver failure is APAP [9]. APAP is a widely used analgesic and antipyretic drug which is very well tolerated when taken at recommended doses (up to 4 g/day). However, when these doses are exceeded or due to a decreased capacity to adequately deal with APAP (poor nutrition, alcohol consumption, etc.) our ability to safely remove APAP becomes impaired (Figure 1). At doses > 4 g/day APAP, the phase II metabolism pathways of sulfation and glucuronidation, which account for ~95 % APAP metabolism at therapeutic doses, become overwhelmed. Increased amounts of APAP undergoes oxidative metabolism by CYP450s to *N*-acetyl-*p*-benzoquinone imine (NAPQI) the potentially toxic reactive intermediate. Cellular defence to this reactive metabolite involves conjugation to glutathione (GSH). However, at doses > 4 g/day, intracellular stores of GSH becomes depleted and NAPQI is free to bind cellular proteins, initiating a cascade of events which ultimately results in hepatotoxicity, localising in the centrilobular regions of the liver. APAP is commonly used in research as a model hepatotoxicant due to the wealth of information available on it (pharmacokinetics, metabolism, toxic effects, etc.), its ability to induce similar toxicity in animal models and low cost. All these factors, and more, make APAP an ideal chemical to use as a tool to gain an understanding of the molecular and cellular events that occur during the progression of hepatotoxicity, including the release of biomarkers.

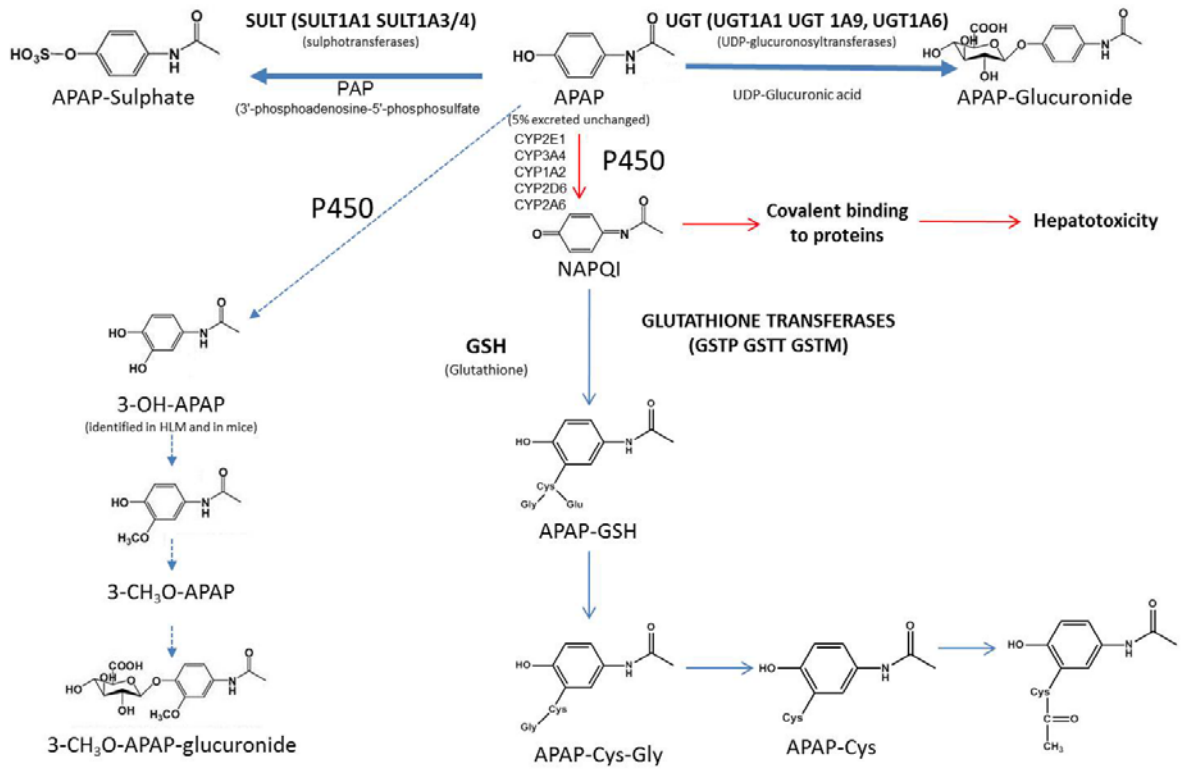

Figure 1. Paracetamol metabolic pathway. APAP is metabolised to a variety of non-toxic metabolites (blue arrows), predominantly APAP-sulfate and APAP-glucuronide at non-toxic doses. However, at toxic doses (red arrows), APAP is metabolised by CYP450s to NAPQI which has the potential to bind cellular proteins and cause hepatotoxicity once GSH is depleted.

1.4 Problems in gaining a mechanistic understanding in toxicology

To gain an understanding of the mechanistic reasons for a toxic event, an acute dosing regimen is often used. In such a scenario, a very high dose of the toxic compound (e.g. APAP) is administered as one single dose via a relevant route (oral, I.V., etc.). In such cases, there can be a compression of toxic events with a very narrow window for their detection (Figure 2). We have found, that acute dosing of animals can lead to a compression of events of toxicological significance. For example, acute dosing of fed mice with hepatotoxic levels of paracetamol, led to a very short period (1-1.5 hours) where cell death via apoptosis was the initial toxicological consequence, prior to overt necrosis [10]. This needed to be verified extensively as this finding was not known to occur in APAP toxicity in mice, leading to further animal usage. The narrow window for detection of apoptosis in this instance shows why such findings had previously been missed, most likely due to sampling time points that did not fall within this narrow window. The need for finer control over serum/plasma drug levels (C_{max}, AUC, P_{ss}, *etc*) in animal models has become crucial, particularly as acute dosing regimens can compress or suppress events of toxicological, and possibly therapeutic, significance. Consequently, it was decided that chronic infusion and longitudinal sampling would help stratify the

pharmacokinetics with biological endpoints, defining the toxicology as threshold-, exposure- or chronically-mediated.

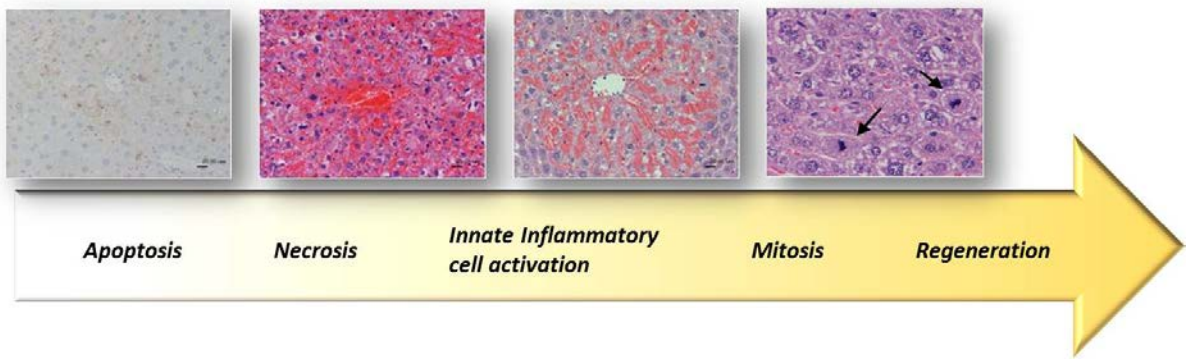

Figure 2. Steps in the progression of APAP toxicity in mice. Mice administered 530 mg/kg APAP displayed a progression of toxic events beginning with apoptosis and ending in regeneration, with the duration of each process varying considerably [10].

2. Development of a new toxicity model

2.1 Continuous intravenous infusion

A typical repeat dose oral dosing regimen in man aims to maintain drug-serum/plasma levels within a 'therapeutic window'. When this repeat-dose scenario is replicated in rodents, the drug-serum/plasma profile is often markedly different (Figure 3). One reason for this difference is rodents eliminate compounds more rapidly than humans, for example the non-steroidal anti-inflammatory drug piroxicam has a $t_{1/2}$ of 45 hours in humans and 6-16 hours in rats, depending on sex [7, 11]. This can in some instances lead to rodents experiencing a 'drug holiday' which is not present in man. The use of CII is hoped to bridge this gap by eliminating this 'drug holiday' and developing a method where drug exposure is more representative of the human situation. This CII model involves the placement of a catheter into the femoral vein of an anaesthetised rat through which drug can be administered at a controllable rate. At the same time a second catheter is placed in the jugular vein from which blood samples can be taken without the need for animal handling, repeated needle pricks and associated animal stress. Each animal acts as its own control as multiple samples can be taken from the same animal, including a pre-dose sample. Using this method, a complete picture of the pharmacokinetics (PK) and toxicity of a compound can be obtained from one animal, thereby leading to an estimated 66 % reduction in animal use and reduction in inter-animal variation. For example, in a typical acute dosing model 6 animals would be used per dose or time point with a higher degree of variation expected (20 %). This compares with 2 animals per dose or time point in a chronic infusion model where drug exposure (and subsequent toxicity) can be more tightly

controlled and a reduction in variation (2-4 %) can be achieved as each animal acts as its own control (Figure 4).

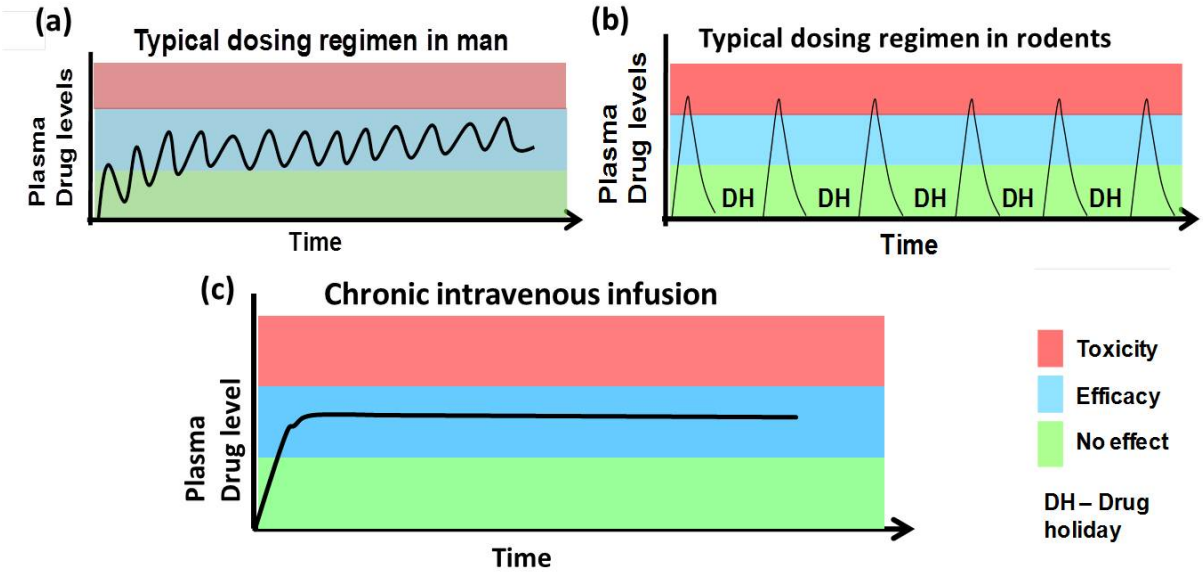

Figure 3. Schematic representation of plasma-drug profiles in man and rodent following repeat dose regimens and chronic infusion regimen. In man following repeat dosing (a) plasma –drug levels remain within the therapeutic window despite minor fluctuations, in rodents (b) more rapid elimination makes replicating the human situation more difficult. Through chronic intravenous infusion (c) more consistent plasma-drug levels may be achieved, which are more representative of the human situation.

Dosing model	Parameters measured	Degree of change required for biological significance	Variation	Power	Number of animals per condition
Acute dosing	1.Biomarkers 2. Toxicity markers	50%	20%	85%	**6**
Chronic infusion	1.Biomarkers 2. Toxicity markers	50%	2-4%	85%	**2**

Figure 4. Reduction in animal usage (by 66 %) in chronic infusion model of toxicity.

In addition, this CII toxicity model has the potential for use as a tool to gain a better mechanistic understanding of the steps involved in the progression of toxicity. In theory, by administering a drug at a slow rate over a long period of time we can slow the progression of disease and untangle the steps involved in its progression more easily. This contrasts with the more difficult task of trying to untangle events that have been compressed by acute bolus dosing. To gain an insight into the steps

involved in the progression of toxicity we will utilise predictive and informative biomarkers (novel and conventional) of toxicity.

Chronic longitudinal analysis will allow the generation of *before-during-after* type of data sets and can give valuable information such as the

1. Steady state pharmacokinetics of the drug – reflecting the clinical situation
2. Side-step drug holiday issues in animal models on daily dosing regimes
3. Appearance and time course of clinically relevant parameters
4. Reduction of experimental variation and increase in experimental power

In addition, it is hoped to be used as a tool for

1. Biomarker identification and validation
2. Dynamic changes in combinations of biomarkers and association patterns
3. Identification of transition points or switch between pathological states – eg. apoptosis to necrosis

2.2 Introduction to the problem-Previous chronic infusion studies and their results

In a preliminary study, performed in conjunction with AstraZeneca, APAP was infused via a femoral vein catheter; 36 mg/kg/hr for 48 hr (6 mg/ml, 6 ml/kg/hr) to male Wistar Hannover (HsdHan:WIST) rats (n=3). Infusion of APAP at a constant rate failed to produce steady state drug-serum levels over the duration of the experiment (Figure 5). Drug-serum APAP level increased steadily until 30 hr at which time there was a shift to increased elimination of parent compound. This increase in elimination has been attributed to an adaptive response; however the precise reasons remain unknown. Previous modelling approaches have attempted (Figure 6) to model the pharmacokinetics of APAP when administered by CII. However, these both under-predicted the drug-serum level and failed to replicate drug-serum profile. It is clear that this more basic mathematical model is not capable of taking into account adaptive processes, which in the case of APAP, have a profound effect on drug-serum a profile.

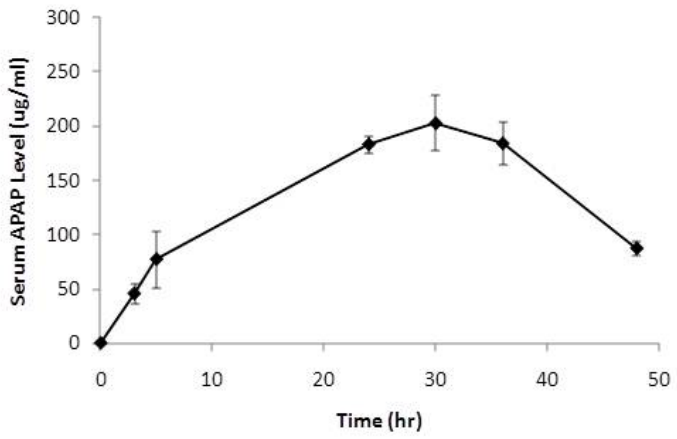

Figure 5. Serum APAP levels over 48 hours. Quantification of serum-APAP concentration of 3 male rats administered APAP at 36 mg/kg/hr for 48 hr (6 mg/ml, 6 ml/kg/hr) at 0, 3, 5, 24, 30, 36 and 48 hours after administration commenced.

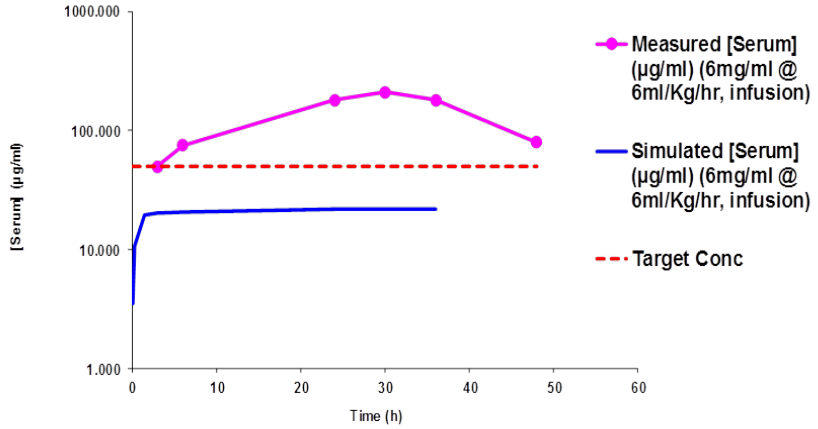

Figure 6. Simulated, Target and Measured serum-APAP concentrations. Computer simulated (blue) serum-APAP concentration both under-predicted the target (red) and measured (purple) drug-serum level and failed to replicate the measured drug-serum profile.

In addition to the unpredicted pharmacokinetics, administration of APAP via CII induced hepatotoxicity which was not expected. Increases in serum alanine transaminase (ALT), high mobility group box one protein (HMGB1) and ophthalmic acid and decreased hepatic GSH and presence of centrilobular necrosis in terminal samples from all treated animals indicate APAP induced hepatotoxicity, evident in the latter stage of administration (Figure 7).

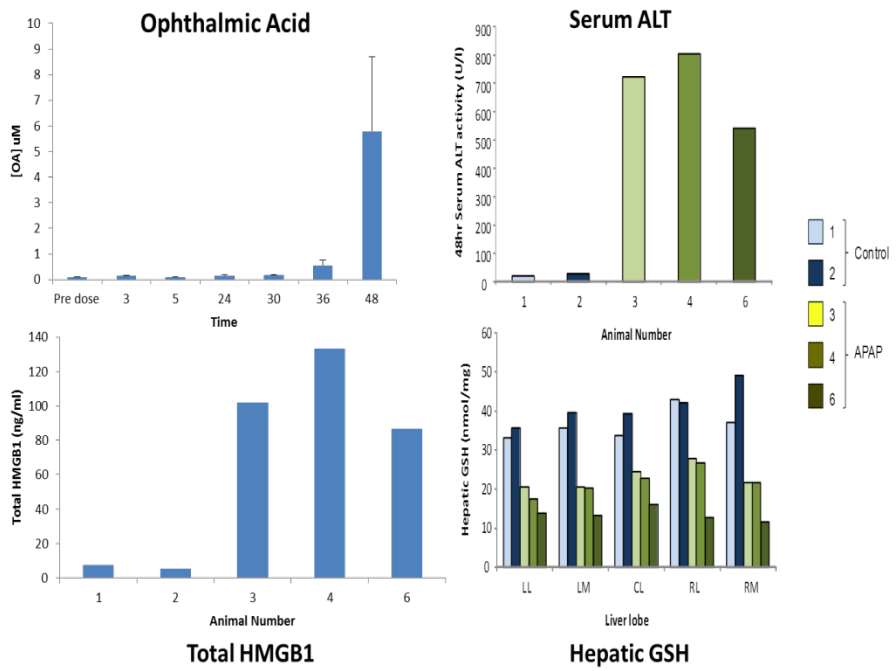

Figure 7. Evidence of hepatotoxicity in treated animals 48 hours after administration commenced. Ophthalmic acid increased in treated animals at 48 hours only (relative to pre-dose sample), Serum ALT elevations at 48 hours only (relative to control), Total HMGB1 elevations at 48 hours (relative to control) and decrease in hepatic GSH at 48 hours (relative to control).

It is evident from these pharmacokinetic and initial modelling results that there are certain additional factors that need to be taken into account when considering the APAP drug-serum profile and the attainment of a steady state, which were not considered in the more simplified model mentioned previously (Figure 6). Chronic infusion experiments are technically demanding, lengthy and expensive, consequently, maximizing experimental design is a priority to ensure most efficient data generation and to minimise animal usage. It is hoped that through the generation of a mathematical model to predict accurately the serum profile of APAP in the circulation we may be able to test possible reasons for this profile and thereby direct experimentation to confirm these hypotheses and/or alter our infusion parameters in order to achieve a steady state.

2.3 Possible explanations for the pharmacokinetic profile

Several possible reasons for the unpredicted serum profile of APAP following CII have been considered separately to this document with the three thought to most probable taken forward for inclusion/consideration in modelling the serum profile of APAP:

1) Uprated GSH cofactor production, increasing the amount of absorbed APAP
2) Higher efflux transporter activity
3) Higher CYP450 expression

3. Parameter Selection

3.1 Construction if PBPK Model

In vitro in vivo extrapolation (IVIVE) is a bottom up technique which aims to simulate pharmacokinetics using *in vitro* data, such as the physicochemical characteristics and intrinsic clearance (CL_{int}) through physiologically-based pharmacokinetic (PBPK) models, which mathematically describe absorption, distribution, metabolism and elimination (ADME).

In the above mentioned fashion, a PBPK model was then constructed to describe the chronic infusion of Paracetamol to the rat given at 3.969 µM/min/kg to investigate different metabolic hypotheses to predict metabolism.

3.2 Rat Model

A flow-limited PBPK model based on the structure with the parameters provided by International Life Science Institute (1994) were used for the construction of the anatomy of the rat. A three-compartment model (blood, liver, and the rest of the tissues) was developed for Paracetamol, with the assumption that blood and the rest of the tissue compartments are in equilibrium with one another and metabolism occurred via the liver. All physiological parameters were obtained from the literature as shown in Table 1. Differential equations based on mass conservation principles were derived for each compartment. Tissue to blood partition coefficients were calculated using experimentally- derived values from Poulin et al., 2002 [12]. After derivation, all equations were coded into MatLab (MathWorks, version 2012b) using the equation solver ode15s. This PBPK model was coupled with Ochoa model (which has the mathematical equations of the different possible pathways used for the clearance of paracetamol from the liver) to study further about the exact pathway of the metabolism of Paracetamol.

Table 1. Parameters for Adult Male F-344 Rats and corresponding references in the PBPK model.

Parameter		Description	Value/Expression	Reference
	Age	Age in weeks	10	-
	Weight	Weight in Kg	(16.2*Age+86.80)/1000	[13]
Weights of Individual Organs (in Kg)	Bones	Bones	4.77*Weight/100	
	Brain	Brain	0.57*Weight/100	
	StomachW	Stomach	0.46*Weight/100	
	Intestines	Gut	2.24*Weight/100	
	Heart	Heart	0.33*Weight/100	
	Kidneys	Kidneys	0.73*Weight/100	
	Liver	Liver	3.66*Weight/100	
	Lungs	Lungs	0.5*Weight/100	
	Muscle	Muscle	40.43*Weight/100	
	Skin	Skin	19.03*Weight/100	
	Spleen	Spleen	0.2*Weight/100	
	Pancreas	Pancreas	0.32*Weight/100	

	Adipose	Adipose Tissue	0.035*(Weight*1000)+0.205)*(Weight)/100	
Blood Flow Rates	QC_total	Cardiac Output	0.235*(Weight^0.75)*60	
	Qha	Hepatic Artery	0.021*QC_total	
	Qpv	Portal Vein	0.153*QC_total	
Volumes of Organs	LiverV	Liver	Liver	
	RestV	Rest of the organs	Weight-LiverV	
	BloodV	Blood	0.016*Weight	
Drug Parameters	fu	Fraction Unbound	1	-
	pKa	Acid-base dissociation constant	9.38	http://www.drugbank.ca/drugs/DB00316
	Kpc	Logarithmic value of octanol to water partition coefficient	0.46	
	R	Blood to plasma ratio	1	-
Volume of Distribution	PC	Octanol to water partition coefficient	10^Kpc	[12]
	D_vo_w	Partition Coefficient of nonionized to ionised species of adipose tissue	10^(1.115*Kpc-1.35)	
	fut	Fraction unbound in tissues	1/(1+(((1-fu)/fu)*0.5))	
	EP	Erythrocyte to Plasma ratio	(R-(1-0.45))/0.45	

3.3 Volume of distribution

Volume of Distribution (V_d) is one of the important factors that has to be taken into consideration for the construction of a PBPK model. V_d is the apparent volume in which the drug is assumed to be dissolved. When the V_d is at steady state (SS) it may also be referred to as V_{ss} as seen in equation 1. V_d (or V_{ss} in this case) of a drug can be computed for any organism with the following formula:

$$V_{\mathrm{ss}} = (\Sigma V_{\mathrm{t}}^{*} P_{\mathrm{t:p}}) + (V_{\mathrm{e}}^{*} E{:}P) + V_{\mathrm{p}}$$

Equation 1

where E:P is the erythrocyte to plasma partition coefficient of the drug, $P_{t:p}$ is the tissue to plasma partition coefficient, V_e is the volume of erythrocytes, V_p is the volume of plasma, V_{ss} is the volume of distribution at steady state and V_t is the volume of the tissue.

V_d is influence by drug specific characteristics such as pKa, blood to plasma ratio (R), fraction of the unbound drug in plasma (fu), the nature of the drug (acidic, basic, neutral or zwitterionic).

Calculation of Volume of Distribution: The formulae shown below (Equation 2) are used for the calculation of the tissue to plasma partition coefficient of each tissue. The data for the below variables are given in Table 1

$$P_{\mathrm{t:p\,adipose}} = \frac{[D_{\mathrm{vo:w}}^{*} \times (V_{\mathrm{nlt}} + 0.3 \times V_{\mathrm{pht}})] + [1 \times (V_{\mathrm{wt}} + 0.7 \times V_{\mathrm{pht}})]}{[D_{\mathrm{vo:w}}^{*} \times (V_{\mathrm{nlp}} + 0.3 \times V_{\mathrm{php}})] + [1 \times (V_{\mathrm{wp}} + 0.7 \times V_{\mathrm{php}})]} \times \frac{fu_{\mathrm{p}}}{1}$$

$$P_{\mathrm{t:p\,nonadipose}} = \frac{[P_{\mathrm{o:w}} \times (V_{\mathrm{nlt}} + 0.3 \times V_{\mathrm{pht}})] + [1 \times (V_{\mathrm{wt}} + 0.7 \times V_{\mathrm{pht}})]}{[P_{\mathrm{o:w}} \times (V_{\mathrm{nlp}} + 0.3 \times V_{\mathrm{php}})] + [1 \times (V_{\mathrm{wp}} + 0.7 \times V_{\mathrm{php}})]} \times \frac{fu_{\mathrm{p}}}{fu_{\mathrm{t}}}$$

Equation 2

Table 2. Physiological Parameters for Volumes and Composition of Tissues of Adult Male rats and Humans Used for Predicting V_{ss}^{α}. All these values are used for the calculation of the volume of distribution which is given by Equation 1.

	Tissue Volume		Tissue Composition (Volume Fraction of Wet Tissue Weight)						
	(Fraction of Body Weight; L/kg)		Water (V_w)		Neutral Lipids (V_{nl})		Phospholipids (V_{ph})		Extracellular (Interstitial) Space (V_{eis})
Tissues	Rat	Human	Rat	Human	Rat	Human	Rat	Human	Rat
Adipose	0.0761	0.11957	0.12	0.18	0.853	0.79	0.002	0.002	0.175
Bone	0.041476	0.085629	0.446	0.439	0.0273	0.074	0.0027	0.0011	0.42
Brain	0.0057	0.02	0.788	0.77	0.0392	0.051	0.0533	0.0565	0.162
Gut	0.027	0.0171	0.749	0.718	0.0292	0.0487	0.0138	0.0163	0.39
Heart	0.0033	0.0047	0.779	0.758	0.014	0.0115	0.0118	0.0166	0.156
Kidney	0.0073	0.0044	0.771	0.783	0.0123	0.0207	0.0284	0.0162	0.346
Liver	0.0366	0.026	0.705	0.751	0.0138	0.0348	0.0303	0.0252	0.159
Lung	0.005	0.0076	0.79	0.811	0.0219	0.003	0.014	0.009	0.484
Muscle	0.404	0.40	0.756	0.76	0.01	0.0238	0.009	0.0072	0.115
Skin	0.190	0.0371	0.651	0.718	0.0239	0.0284	0.018	0.0111	0.462
Spleen	0.002	0.0026	0.771	0.788	0.0077	0.0201	0.0136	0.0198	0.264
Plasma	0.0449	0.0424	0.96	0.945	0.00147	0.0035	0.00083	0.00225	1.00
Erythrocytes	0.0367	0.0347	—	—	—	—	—	—	—

[a]Mean values obtained from a review of the literature. See Appendix for the estimation and references concerning V_t, V_p, V_e, V_w, V_{nl}, V_{ph}, and V_{eis}. Data represent a rat of 250 g and a human of 70 kg.
—, Not used in the present study.

3.4 Compartmental Model

This model consists of only three compartments i.e. the blood, liver and the rest. The chronic infusion is given at the rate of 3.969 uM/min/Kg of rat. It is assumed that the blood and the rest compartments are in equilibrium and the direction of the blood flow is from blood to rest, rest to blood, blood to liver and liver to blood again.

Parameter	Description	Initial Value
BloodP	Plasma Compartment	0
RestP	Tissue Reservoirs	0
LiverP	Metabolism Compartment	0

Differential Equations

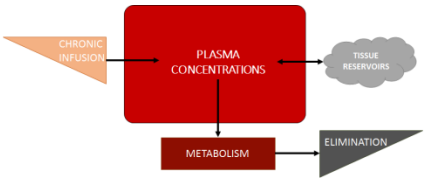

1. $\frac{d}{dt} BloodP = 3.396 * weight + (Qha + Qpv) * \frac{LiverP}{LiverV} + (QC_{total} - Qha - Qpv) * \frac{RestP}{RestV} - QC_{total} * BloodP$
2. $\frac{d}{dt} LiverP = (Qha + Qpv) * \left(\left(\frac{BloodP}{BLoodV}\right) - \left(\frac{LiverP}{LiverV}\right)\right) - Metabolism\ (Ochoa\ Model)$
3. $\frac{d}{dt} RestP = (QC_{total} - Qha - Qhv) * \left(\left(\frac{BloodP}{BLoodV}\right) - \left(\frac{RestP}{RestV}\right)\right)$

This PBPK model is coupled with the metabolism in the liver given using the Ochoa Model.

4. Mathematical Model Development

4.1 Reduction of the Ochoa Model

The mathematical complexity and size of the Ochoa model [14]was reduced by removing aspects of the model relating to the intracellular unspecific binding of acetaminophen (APAP) and metabolites to lipids and proteins. Subsequently, associated processes, including those describing the synthesis of Reactive Oxygen Species (ROS) and Reactive Nitrogen Species (RNS) were also removed. The unspecific binding of APAP with lipids and proteins was not thought to have a significant influence on the overall metabolic process being focused on. An example form of the equations of which the Ochoa model [14] is composed, describing the rate of change of a concentration (c_i) with time (t) is shown in Equation 3.

$$\frac{dc_i}{dt} = r_1 - r_2,$$

Equation 3

here r_1 and r_2 may be functions of c_i and/or concentrations of other metabolites c_j contributing to the particular reaction pathway.

In order to reduce the system of model equations we set the reaction rates associated with each of these processes identified to zero in order to remove their contribution to the model system. Figure 8 shows a schematic of the full model and Figure 9 outlines the reduced version of the model which was used.

The reduced model was simulated in order to ensure that it replicated physiologically sensible and expected behaviour and that the behaviour exhibited was sufficiently similar to that of the full model. In Figure 10 results obtained from the reduced model upon application of a 1 mg single bolus dose are shown. We can see from these results that the concentration of APAP in the cell and media decreases over time following the initial bolus dose. The level of APAPS initially increases as APAP concentration becomes high inside the cell and then starts to decrease as APAP begins to be removed and its concentration in the cell decreases. Similarly, the concentration of GSH, involved in the elimination of NAPQI, decreases as APAP concentration in the cell declines, and then begins to replenish again once there is a zero concentration of APAP in the cell and hence no further NAPQI production.

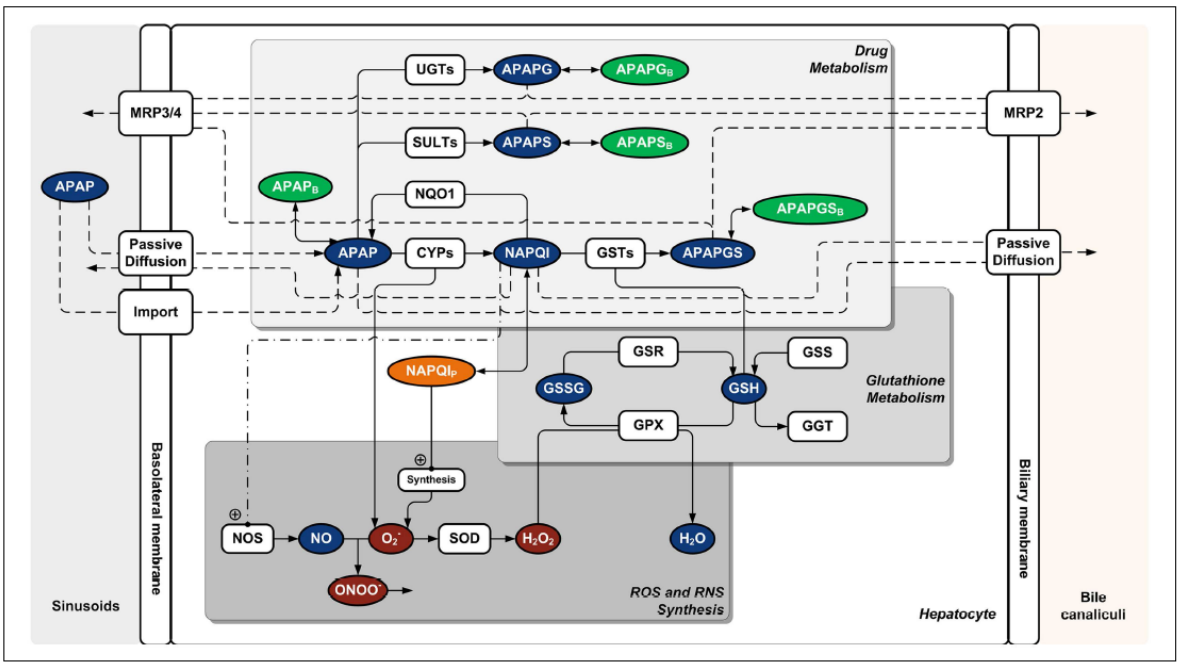

Figure 8. Full description of cellular metabolic network model for acetaminophen metabolism and toxicity as proposed by Ochoa et al. [14].

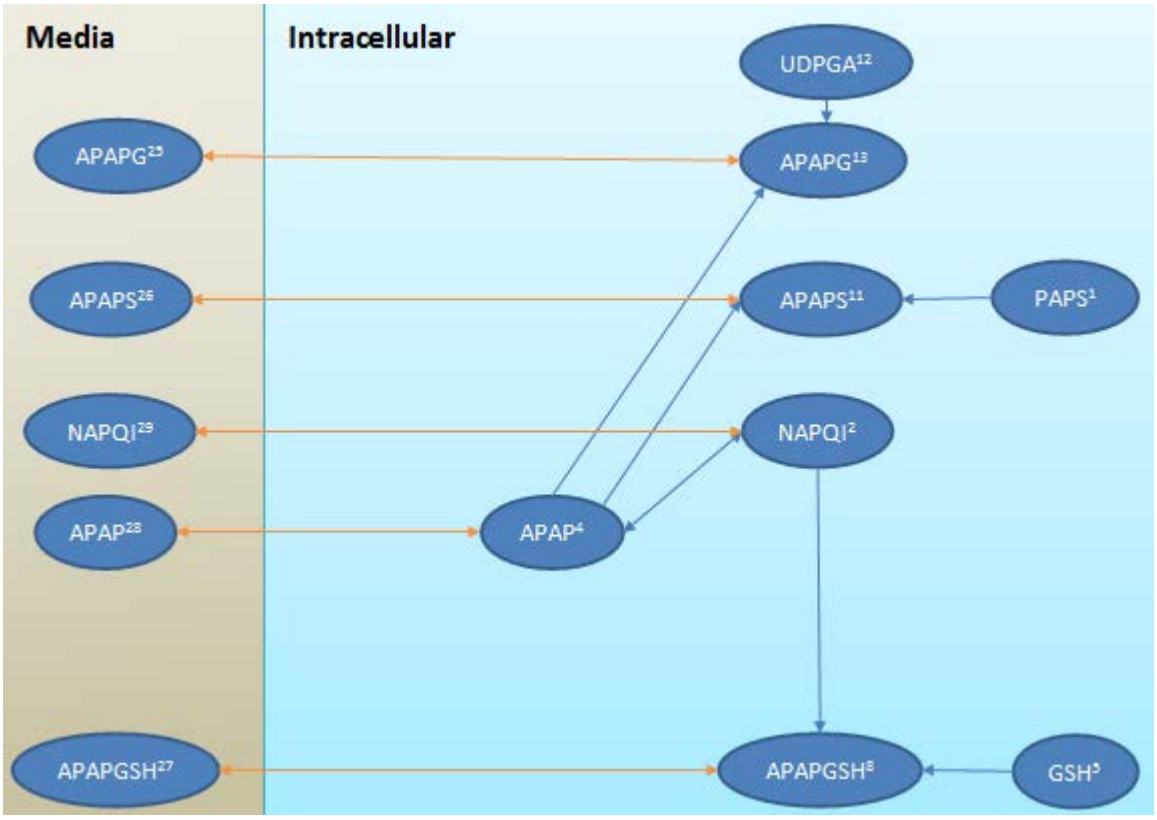

Figure 9. Reduced cellular metabolic network model for acetaminophen metabolism with protein and lipid binding and associated processes removed.

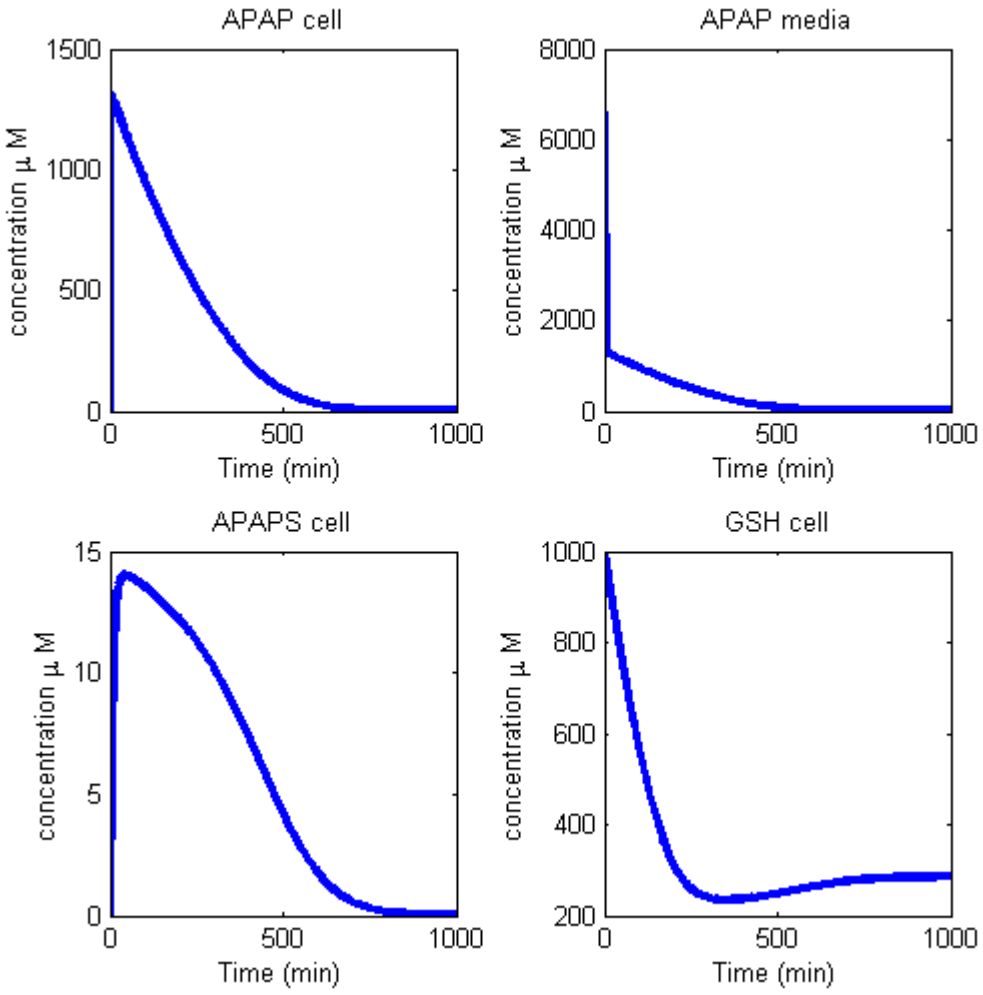

Figure 10. Results from simulation of reduced Ochoa model with 1 mg bolus dose of acetaminophen. APAP cell, APAPS cell and GSH cell being the levels of APAP, APAPS and GSH in the liver cell respectively and APAP Media is the level of APAP in the media.

4.2 Coupling of Ochoa and PBPK Models

The next step was to couple the reduced Ordinary Differential Equation (ODE) model with the PBPK model so to incorporate a more detailed model of acetaminophen interaction. This was achieved through coupling of the PBPK model via the equation describing the level of acetaminophen in the media. Thus, the original equation describing the rate of change of the level of APAP in the media, which relied solely on APAP movement between the intracellular space and the media, was modified to include movement to and from the blood into the liver. Two further equations were added to the Ochoa model formulation to complete the coupling, describing the APAP level in the blood compartment and the compartment representing the rest of the body.

An assumption made in making this coupling is that the volume of the rat liver is 5 % of the volume of the human liver, as the equations in the Ochoa model are based upon human acetaminophen metabolism. This coupled model then allowed us to model chronic drug infusion. We then ensured that the coupled model replicated the expected behaviour of the coupled PBPK model. Figure 11 shows the behaviour exhibited when the model is simulated with chronic infusion of acetaminophen. We see here that the APAP levels in the cell, the blood compartment and the compartment representing the rest of the body increase over time and eventually reach a steady level, as would be expected during chronic infusion. We also see that the level of GSH in the cell is high initially, decreases with increasing APAP concentration in the cell and also reaches a steady level, again as expected.

We next compared these preliminary results from the coupled model with the experimental results which originally motivated this problem. The model prediction of the level of APAP in the blood over time, with the experimental recordings can be seen in Figure 12. We can see from this initial comparison that the model predictions are now overestimating rather than underestimating the measured experimental results but the model is reaching a steady state as we would expect. While we are not yet replicating a shape in which we see a peak followed by a decline in the APAP concentration in the blood, we now have a basis on which we can begin to explore potential adaptive mechanisms to further investigate this system. This will allow us to test plausible mechanisms using the mathematical model before determining those for which it would be of value to explore experimentally.

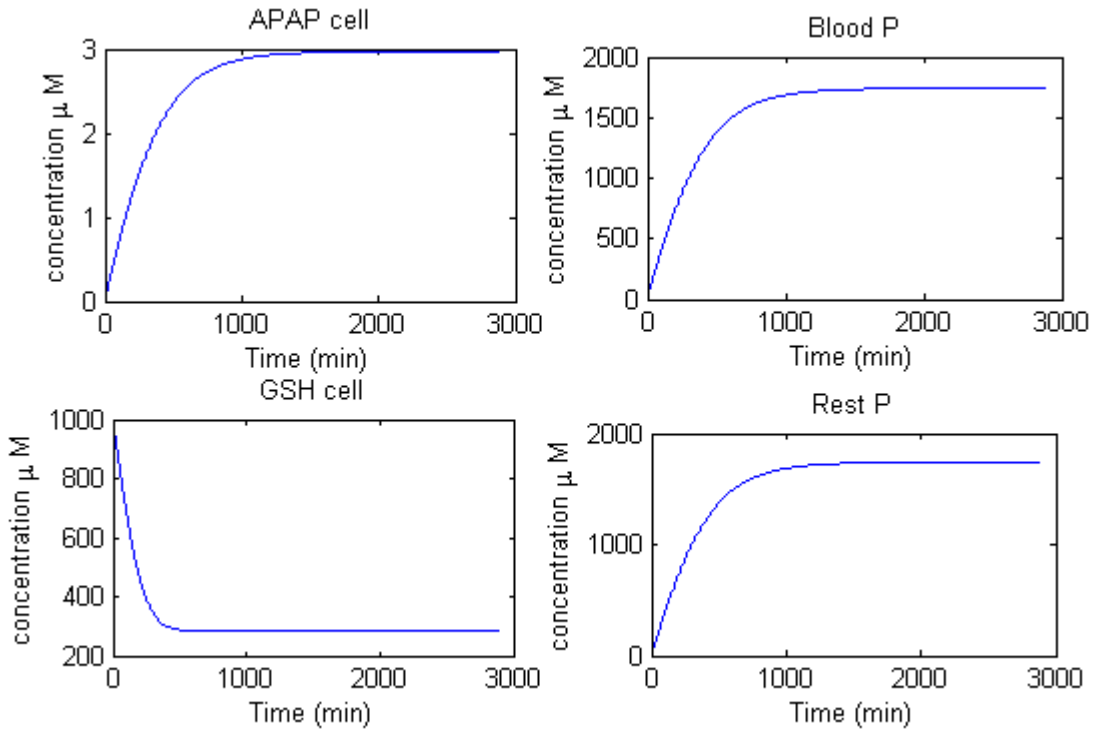

Figure 11. Results of coupled model with chronic acetaminophen infusion, with APAP cell and GSH cell being the levels of acetaminophen and GSH in the liver cell respectively, and Blood P and Rest P being the levels of APAP in the blood compartment and the rest of the body respectively.

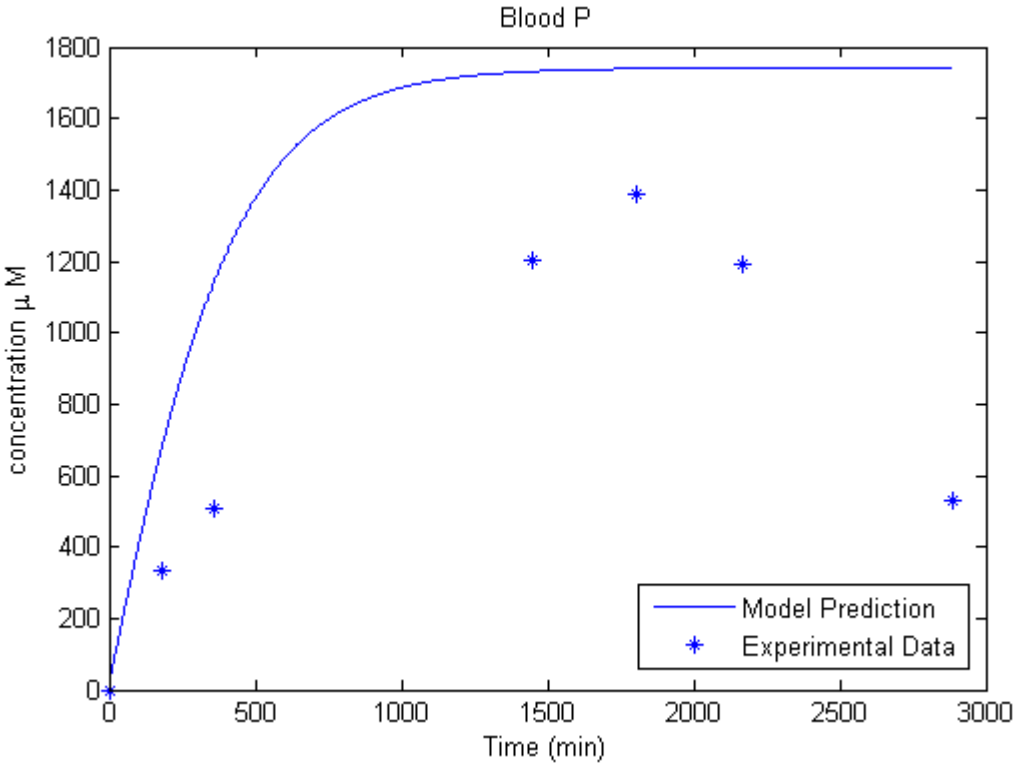

Figure 12. Model prediction of concentration of APAP in the blood over time as compared to the concentration determined from experimentally recorded samples following chronic drug infusion.

4.3 Exploring Adaptive Mechanisms

We investigated three scenarios which were thought could be plausible explanations for the observed trend in APAP concentration. This was done by adapting the appropriate parts of the model described above and seeing if any resulted in an eventual decrease in APAP concentration instead of a steady state.

The first adaptation was motivated by a potential nonlinear dependence of GSH production on NAPQI concentration. It was proposed that, instead of GSH being produced at a constant rate in the presence of NAPQI, the production rate would at first increase with NAPQI concentration, before decreasing after a certain threshold of NAPQI had been reached. This corresponded to the following change in the production term in the ODE for GSH concentration:

$$P_{\mathrm{GSH}} \quad \longmapsto \quad K_1 + \frac{K_2 C_{\mathrm{NAPQI}}}{K_3 + C_{\mathrm{NAPQI}}^2},$$

Equation 4

where p_G is the original constant rate of production of GSH, c_{NAPQI} is the concentration of NAPQI, and K_1, K_2, K_3 are constants chosen to obtain the desired peaked dependence. A graph of this new term versus NAPQI concentration can be seen in Figure 13. Biologically, it is expected that the change in GSH production rate would occur with a time delay of around 5 hours. However, including a time delay in our model was found to be computationally expensive and so for the purposes of this work we instead switched from the constant production rate to the new production rate when a certain threshold value (chosen to be that achieved after around 5 hours) of NAPQI had been reached. Results from this adaptation were obtained using the reduced Ochoa model, with an added flow into and out of the media to simulate chronic infusion, and can be seen in Figure 14. From this we see that this adaptation significantly decreased the GSH concentration in the cell. However, it had no significant effect on the APAP concentration in the media or in the cell, and in particular did not reproduce the trend found in experiments.

The second adaptation explored the possibility that the observed trend in APAP concentration could be due to a changing rate of transport of metabolites out of the cell as a result of increasing NAPQI concentration. The suggested trend was similar to that in the first adaptation, and the corresponding ODEs were modified as demonstrated in Equation 4. Again, a time delay for this change would be expected physically, but we imposed a threshold NAPQI concentration for the reasons discussed above. This adaptation was again tested on the reduced Ochoa model, but produced unrealistic results and therefore needs further consideration.

The third and final adaptation we considered was that the experimental findings could be due to increased expression of CYP450 above a certain NAPQI concentration. This simply corresponded to increasing the maximum production rates of the appropriate enzymes in our ODE model. We were able to test this hypothesis on the coupled ODE-PBPK model, and results can be seen in Figure 15. As this figure shows, we were able to produce a decrease in APAP concentration after a certain time. Due to the sudden switch in behaviour at the threshold NAPQI concentration imposed by our simplified model, the resulting graphs have a sharp peak which is unrealistic. However, the fact that this shows the same qualitative behaviour as experiments is promising, and we believe that including a time delay in the model may smooth out this peak and produce more realistic results.

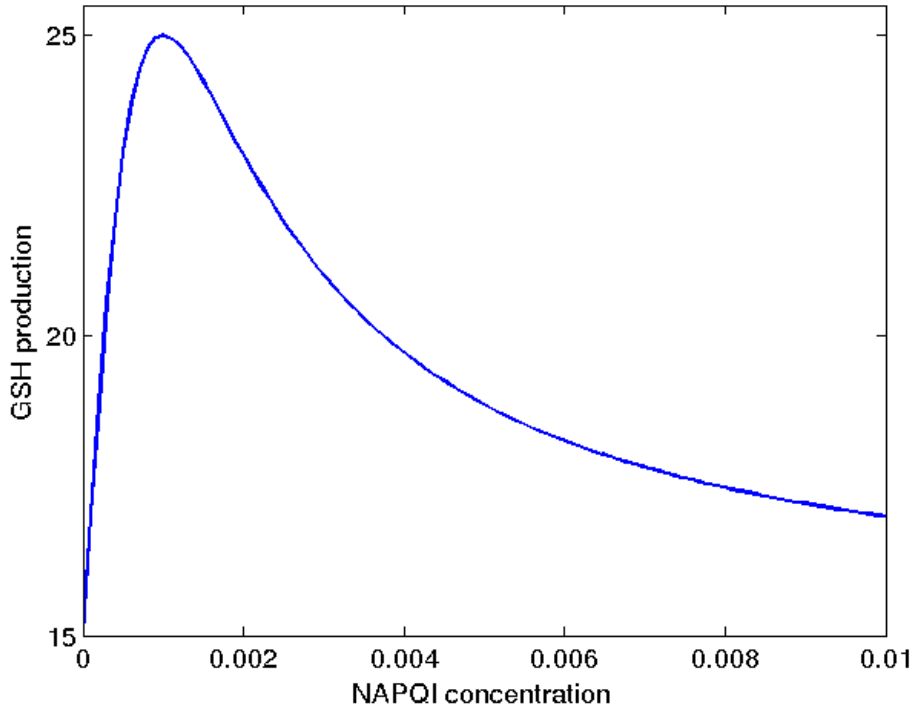

Figure 13. Example of the proposed nonlinear dependence of GSH production on NAPQI concentration as described in Equation 4.

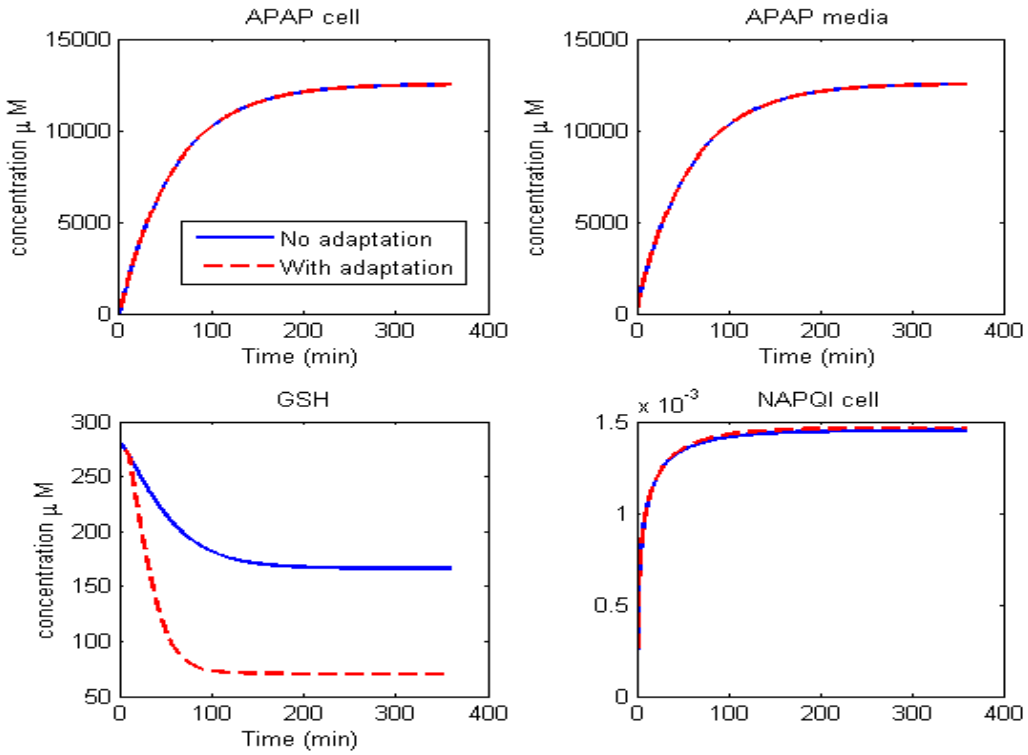

Figure 14. Results from the first adaptation, where there is a nonlinear dependence of GSH production on NAPQI concentration. APAP cell, GSH and NAPQI are the levels of APAP, GSH and NAPQI in the liver cell respectively and APAP Media is the level of APAP in the media.

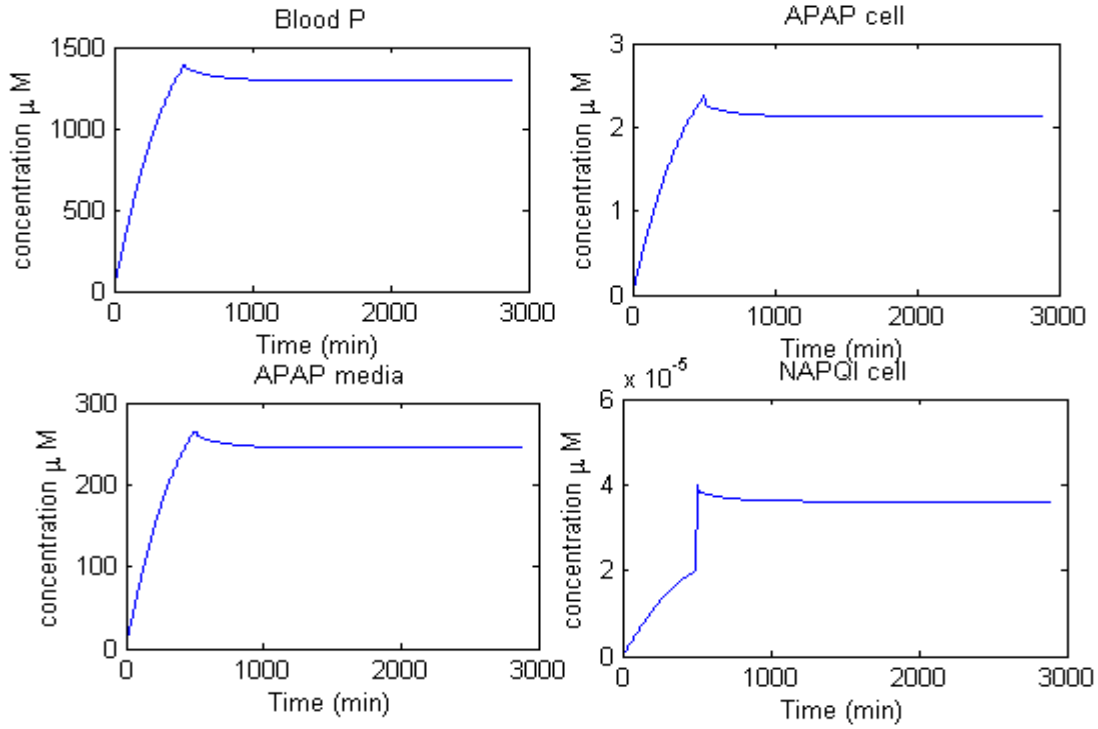

Figure 15. Results from the third adaptation, where there is assumed to be increased expression of CYP450. APAP cell, and NAPQI cell are the levels of APAP and NAPQI in the liver cell respectively, Blood P is the level of APAP in the blood compartment, and APAP media is the level of APAP in the extracellular space in the liver.

5. Discussion and Conclusions

CII of APAP at 36 mg/kg/hr for 48 hr to male *Wistar* Hannover rats (HsdHan:WIST) failed to achieve steady-state drug-serum levels due to an unidentified adaptive response. The drug-serum profile was not predicted by previous mathematical models as these failed to take into account an adaptive response.

Our preliminary model has included three possible adaptive responses which could be responsible for the APAP-serum profile. Of these, one was identified as a possible mechanism by which APAP concentration in the blood could be changing; increased CYP450 expression above a certain NAPQI concentration. Results of this mechanism showed a sudden switch in behaviour at the threshold NAPQI concentration imposed by our simplified model, the resulting graphs gave a sharp peak which is biologically unrealistic. However, the fact that this shows the same qualitative behaviour as experiments is promising, and we believe that including a time delay in the model may smooth out this peak and produce more realistic results.

Future work will focus on refining the model, with the inclusion of adaptation time delays to equations when exploring the possible adaptation responses. This was found to be computationally expensive in MATLAB but may provide more biologically comparable results. We will also investigate additional explanations for the pharmacokinetic profile to ascertain if any of these may have an impact on the profile. Some model assumptions and non-rat parameterisation have been included in the model which needs to be investigated further to confirm these are biologically correct when modeling CII in the rat. With the inclusion of the aforementioned, the model may be taken forward for publication and used in experimental design of future CII studies.

6. 3Rs Impact

Toxicity issues account for ~21% drug attrition during drug development and current safety testing strategies require considerable animal use. A mechanistic understanding of the molecular and cellular events that culminate in whole organ toxicity underpins development of novel drug safety assessment strategies. Current models for safety testing are limited by intrinsic differences between animal and man with respect to how drug levels in the blood are maintained. Specifically, the rapid *in vivo* elimination of drugs in rodents results in qualitative and quantitative differences in pharmaco-toxicological endpoints and confounds comparisons to the human setting. If accurate predictors of toxicity can be used to identify early events in the toxicity process, then safety testing can be done without allowing the animal to experience the toxic events, thereby refining experimental design.

The combination of CII and automated blood sampling gives the possibility to obtain a complete pharmacokinetic and/or toxicity profile from each animal. Multiple samples can be taken from each animal over the duration of the experiment, which reduced the need for rodent subgroups culled at interim time points. In addition, each animal can act as its own control due to pre-dose sampling, which reduced the number of concurrent control animals required. Thus, through this method it is estimated that a 66 % reduction in animals can be achieved with variation of 2-4 %.

Through our mathematical model we have identified one possible explanation for the unpredicted pharmacokinetic profile which allows a more targeted approach to be taken experimentally, focusing more on key areas of importance which may be significant in altering the plasma level of APAP. This will directly allow a reduction in the number of animals used to investigate why these perturbations are occurring as unrealistic avenues can be eliminated from the experimental process. It will also allow experiments to be refined to identify key stages in these perturbations, thereby refining the experimental process to minimise the number of animals used to understand these perturbations. Critically, this model will aid in experimental design of future CII studies to predicting serum-drug levels. This will be key to designing studies where only minimal/early stage toxicity is present. Thereby making the investigation of mechanistic biomarkers of early stages of toxicity more easily investigated, with fewer animals required and improved animal health during studies.

References

1. Lazarou, J., B.H. Pomeranz, and P.N. Corey, *Incidence of adverse drug reactions in hospitalized patients: a meta-analysis of prospective studies.* JAMA, 1998. **279**(15): p. 1200-5.
2. Lasser, K.E., et al., *Timing of new black box warnings and withdrawals for prescription medications.* JAMA, 2002. **287**(17): p. 2215-20.
3. Ostapowicz, G., et al., *Results of a prospective study of acute liver failure at 17 tertiary care centers in the United States.* Ann Intern Med, 2002. **137**(12): p. 947-54.
4. Andersen, M.E. and D. Krewski, *Toxicity testing in the 21st century: bringing the vision to life.* Toxicol Sci, 2009. **107**(2): p. 324-30.
5. HomeOffice, *Statistics of Scientific Procedures on Living Animals, Great Britain 2011*, 2012, The Stationery Office: LONDON. p. 41-44.
6. Igarashi, T., *The duration of toxicity studies required to support repeated dosing in clinical investigation - A toxicologist's opinion.* Timing of Toxicological Studies to Support Clinical Trials, 1994: p. 67-74.
7. Beasley, V., *Absorption, Distribution, Metabolism, and Elimination: Differences Among Species.*, 1999, International Veterinary Information Service (www.ivis.org), USA: Veterinary Toxicology.
8. Park, B.K., M. Pirmohamed, and N.R. Kitteringham, *The role of cytochrome P450 enzymes in hepatic and extrahepatic human drug toxicity.* Pharmacol Ther, 1995. **68**(3): p. 385-424.
9. Verma, S. and N. Kaplowitz, *Diagnosis, management and prevention of drug-induced liver injury.* Gut, 2009. **58**(11): p. 1555-64.

10. Antoine, D.J., et al., *High-mobility group box-1 protein and keratin-18, circulating serum proteins informative of acetaminophen-induced necrosis and apoptosis in vivo.* Toxicol Sci, 2009. **112**(2): p. 521-31.
11. Nau, H., *Teratogenic valproic acid concentrations: infusion by implanted minipumps vs conventional injection regimen in the mouse.* Toxicol Appl Pharmacol, 1985. **80**(2): p. 243-50.
12. Poulin, P. and F.P. Theil, *Prediction of pharmacokinetics prior to in vivo studies. 1. Mechanism-based prediction of volume of distribution.* J Pharm Sci, 2002. **91**(1): p. 129-56.
13. *Physiological parameter values for PBPK models*, 1994, International Life Sciences Institute. p. 1-142.
14. Diaz Ochoa, J.G., *A multi-scale modeling framework for individualized, spatiotemporal prediction of drug effects and toxicological risk.* Frontiers in pharmacology, 2012. **3**(204).